Catalysis Today 157 (2010) 137–142

Contents lists available at ScienceDirect

Catalysis Today

journal homepage: www.elsevier.com/locate/cattod

Role of dispersion of vanadia on SBA-15 in the oxidative dehydrogenation of propane

Philipp Gruene, Till Wolfram, Katrin Pelzer, Robert Schlögl, Annette Trunschke*

Department of Inorganic Chemistry, Fritz Haber Institute of the Max Planck Society, Faradayweg 4-6, D-14195 Berlin, Germany

ARTICLE INFO

Article history:
Available online 14 April 2010

Keywords:
Oxidative dehydrogenation
Propane
Propene
Silica supported vanadia
Vanadia dispersion
SBA-15

ABSTRACT

A series of vanadia catalysts supported on the mesoporous silica SBA-15 are synthesized using an automated laboratory reactor. The catalysts contain from 0.6 up to 13.6V atoms/nm^2 and are structurally characterized by various techniques (BET, XRD, SEM, TEM, Raman, IR, UV/Vis). Samples containing up to 3.1V/nm^2 are structurally rather similar. They all contain a mixture of tetrahedral $(VO_x)_n$ species, both monomeric and oligomeric. The ratio of monomeric and oligomeric species depends on the vanadia loading. At the highest loading of 13.6V/nm^2, in addition to tetrahedral $(VO_x)_n$, also substantial amounts of three-dimensional, bulk-like V_2O_5 are present in the catalyst. The structural similarity of the low-loaded catalysts is reflected in their alike catalytical activity during the oxidative dehydrogenation (ODH) of propane between 380 and 480 °C. Propene, CO, and CO_2 are formed as reaction products, while neither the formation of ethene nor acrolein or acrylic acid is observed in other than trace amounts. The activation energy for ODH of propane is ~140 kJ/mol. The catalyst with the highest loading yields varying activation energies for different reaction conditions, which is probably related to rearrangements between bulk-like and dispersed, two-dimensional $(VO_x)_n$. Rather than the monomer to oligomer ratio, the ratio of two-dimensional to three-dimensional vanadia seems to be crucial for the catalytic properties of silica supported vanadia in the ODH of propane.

© 2010 Elsevier B.V. All rights reserved.

1. Introduction

Vanadium oxide is considered one of the most important compounds in metal oxide catalysis [1]. It is used in a variety of important industrial oxidation processes, like the oxidation of SO_2 to SO_3, the oxidation of benzene to maleic anhydride [2] and *o*-xylene to phthalic anhydride [3], or the selective catalytic reduction of NO_x [4]. Additionally, there is a strong interest in selective dehydrogenation (ODH) reactions of light alkanes to the corresponding alkanes [5]. However, only the selective oxidation of n-butane to maleic anhydride has been commercialized using vanadyl pyrophosphate as a catalyst [6]. For smaller alkanes, this catalyst is much less efficient [7]. Therefore, lots of attention has been devoted to the search for improved vanadia-based catalysts for the ODH of ethane and propane [8]. Complementary research has focused on the geometric structure of supported vanadia catalysts and especially how structure can be related to catalytic performance [9–12]. Despite all this effort, the exact nature of the active site remains the topic of controversial discussions.

Highly ordered mesoporous supports with a large surface area allow for the deposition of a large number of well-defined two-dimensional vanadia species, affording precise spectroscopic investigation of their geometric and electronic structure. SBA-15 is a mesoporous silica material with uniform hexagonal channels, a narrow pore size distribution, surface areas above 800 m^2/g, and considerable hydrothermal stability due to a sufficient thickness of the framework walls [13,14]. All these properties make it a preferable support material for model catalysts [15]. Moreover, vanadia supported on SBA-15 has shown considerable catalytic activity in the ODH of propane [16]. While the possibility to tune the mesoscopic properties of SBA-15 by slight modifications in the synthesis makes it a versatile material [13,14], this creates problems in the reproducibility of the support and batch effects are commonly observed.

In this paper, a controlled and reproducible synthesis of well-defined SBA-15 supported vanadia catalysts is described making use of an automated laboratory reactor. The up-scaled SBA-15 batch size is sufficient for the preparation of a series of catalysts with different loadings from the same support. The catalysts are structurally characterized by BET, XRD, SEM, TEM, Raman, IR, and UV/Vis spectroscopy. Their catalytic performance is tested thoroughly in the ODH of propane. It is shown that at low loadings the structural and catalytic properties of the samples vary only moderately. Only at loadings, at which three-dimensional, bulk-like vanadia species coexist, the catalyst shows marked differences in its catalytic behavior.

* Corresponding author. Tel.: +49 30 8413 4457; fax: +49 30 8413 4405.
E-mail address: trunschke@fhi-berlin.mpg.de (A. Trunschke).

0920-5861/$ – see front matter © 2010 Elsevier B.V. All rights reserved.
doi:10.1016/j.cattod.2010.03.014

2. Experimental

2.1. Catalyst synthesis

SBA-15 was synthesized based on an up-scaled original recipe of Zhao et al. [13,14]. The process was automized in a laboratory reactor (LabMax, Mettler-Toledo) that provides precise control of the operating conditions (temperature, pH, stirring rates) and process data recording. In particular, practically no temperature gradients occur within the reaction vessel that allows synthesis of homogeneous, well-defined SBA-15 in large batch sizes. In brief, 36.6 g of the triblock co-polymer $EO_{20}PO_{70}EO_{20}$ (EO = ethylene glycol, PO = propylene glycol, BASF Pluronic P123) were dissolved at 35 °C in 270 ml of doubly distilled water and 1080 ml 2 M HCl, yielding a clear solution after several hours. Subsequently 81 ml of tetraethoxysilane (TEOS, 99+%, Alfa Aesar) were added dropwise. The solution quickly turned cloudy and was stirred for 20 h at 35 °C. After aging for 24 h at 85 °C, the suspension was filtered and washed ten times with distilled water and ethanol over a nutsch filter (frit with porosity 4) and a vacuum flask, stirring the filter cake occasionally. The resulting white powder was dried at 150 °C for 2 h and calcined in static air at 550 °C (heating rate 1.5 °C/min) for 12 h. After cooling down to room temperature, up to 25 g of SBA-15 were obtained.

The subsequent loading of SBA-15 with vanadia was achieved by a grafting/anion exchange procedure [17,18]. The first step consisted of a surface functionalization using 3-aminopropyltrimethoxysilane followed by the protonation of the resulting amine with HCl. Under stirring, the wanted amount of butylammonium decavanadate $[Bu(NH_3)_6V_{10}O_{28}]$ was added to a batch of 10 g functionalized SBA-15 in 300 ml water at room temperature and allowed to undergo ion exchange for 12 h. The resulting yellow powder was filtered, washed, and calcined for 12 h at 550 °C (heating rate 1.5 °C/min). The nominal loadings of the catalysts were 2, 4, 6, 8, and 20 wt% (corresponding to the vanadium content).

2.2. Physical characterization

Surface areas of the prepared samples were measured by nitrogen adsorption/desorption isotherms at −196 °C and standard multipoint BET analysis methods using a physisorption/chemisorption analyzer (AUTOSORB-6, Quantachrome). Before adsorption, the samples were degassed by heating in vacuum to 120 °C for 16 h. Pore size distributions were calculated from the desorption branch of the isotherms applying the NLDFT method in the software package of the AUTOSORB-6.

Morphology studies and shape analysis were performed with SEM using a Hitachi S-4800 instrument with an acceleration voltage of 1.5 kV. For SEM investigations, the sample was deposited on carbon tape.

The pore- and microstructure of the catalyst was investigated by TEM using a Philips CM 200 FEG microscope operated at 200 kV and equipped with a Gatan CCD camera for image acquisition. The specimens were prepared by dry dispersing the catalyst powder on a standard copper grid coated with holey carbon film.

The loading of vanadia on the SBA-15 support was checked both with EDX using the above SEM with an acceleration voltage of 10 kV, and ICP-AES after dissolving the sample in HF.

The pore diameter and wall thickness was also determined by small angle X-ray diffraction using a STOE STADI-P transmission diffractometer, equipped with a primary focusing Ge monochromator (Cu K_α radiation) and a scintillation counter. The presence of large amounts of crystalline V_2O_5 could be excluded by X-ray diffraction using the same diffractometer, but applying a position sensitive detector.

UV/Vis spectra were taken in a Harrick cell of a PerkinElmer Lambda 650 instrument. To avoid saturation on strong resonances the samples were diluted 20-fold with bare SBA-15 from the same batch. Spectra were taken before and after the mixtures were heated to 450 °C, allowed to dry under a stream of synthetic air for 1 h, and cooled to room temperature again. The blank SBA-15 support was used as reference spectrum.

For the Raman spectroscopy, samples were compressed into small plates and introduced into glass pipettes. After heating to 450 °C the pipettes were sealed and allowed to cool. The spectra were taken with a Trivista Raman system using 3 mW of a 488 nm Ar^+ laser.

2.3. Catalytic testing

The catalytic measurements were performed in a linear fixed-bed quartz reactor (6 mm i.d.) at atmospheric pressure. Between 60 and 400 mg of the catalyst, depending on its loading, were diluted with inert SiC in order to improve the heat transfer and introduced into the reactor. Mass transfer limitations were avoided using particle sizes of 200–315 μm. For the measurements of apparent activation energies a stoichiometric ratio of propane to oxygen of 2 was used (29.1% C_3H_8, 14.5% O_2, 56.4% He) and the temperature was varied between 380 and 450 °C in 10 °C steps. In order to compare the selectivity of the different loadings, the total flow of a stoichiometric mixture was varied between 7.7 and 50.8 ml/min at a fixed temperature of 430 °C. The reaction order in oxygen and propane was determined by varying the flow of one component and keeping the other one fixed at a constant total flow. The propane conversion was kept below 10%, ensuring isothermal and differential conditions. The reactor was surrounded by a 20 cm long heating cartridge serving as a source of heat to provide near isothermal operating conditions. Feed and product components leaving the reactor were analyzed by an on-line micro-GC (Varian Micro-GC 4900) with four TCD detectors. The only significant carbon-containing species detected have been C_3H_8, C_3H_6, CO, and CO_2. The carbon balance based on these molecules was within less than 1% exact.

3. Results and discussion

3.1. Catalyst morphology

The synthesis of SBA-15 in an automated lab reactor allows for the preparation of fairly large amounts of the support. Table 1 summarizes the SAXRD, BET, EDX, and ICP-AES results obtained for the support and for five different nominal loadings. 2, 4, 6, 8, and 20 wt% of the decavanadate had originally been added to the functionalized SBA-15. The ICP and EDX results show that these loadings have actually been achieved for all samples quite precisely except the one, which was supposed to contain 20 wt% vanadium. Using incipient wetness impregnation the monolayer surface coverage of vanadia on silica has been proposed to be less than 0.7 atoms/nm^2 and thus lower as compared to other oxide supports. This has been explained by the lower density and reactivity of silica surface hydroxyls [10]. Unlike the incipient wetness method, the grafting/ion-exchange approach includes a thorough rinsing step after the ion exchange. At this point almost all decavanadate that is not directly bond to the support is washed away. In this regard, the ion/exchange method is similar to the controlled grafting process through atomic layer deposition (ALD). Using ALD, of an original V-loading of 21.6 wt% only 9.2 wt% were measured to be present on the final catalyst. However, this loading corresponds to a surface density of 1.91 atoms/nm^2 [19]. In the case of sample 14V/SBA-15 the surface density is much higher with

Table 1
Physical properties of V/SBA-15 catalysts compared to the blank support.

Sample	V-loading ICP (wt%)	V-loading EDX (wt%)	BET (m^2/g)	V[a] atoms/nm^2	Pore[b] diameter (nm)	a[c] (nm)	Thickness of V-layer[d] (nm)
SBA-15	–	–	950	–	7.0	10.85	–
2V/SBA-15	2.3	2.0	459	0.6	6.8	10.63	~0
4V/SBA-15	4.7	4.5	395	1.4	6.8	10.66	~0
SBA-15	–	–	915	–	7.1	10.63	–
6V/SBA-15	6.4	6.3	362	2.1	6.8	10.84	~0.3
8V/SBA-15	8.1	8.9	308	3.1	6.8	10.85	~0.3
14V/SBA-15	13.6		118	13.6	6.5	11.19	~0.6

[a] Based on the ICP and BET.
[b] From the desorption branch of the N_2 physisorption using a DFT approach.
[c] From SAXRD.
[d] V-layer is calculated as half the difference in wall thickness of the loaded catalyst and the blanc SBA-15 sample.

13.6 atoms/nm^2. This value is far above the threshold, after which usually crystalline V_2O_5 is observed. In previous reports using the grafting/ion-exchange method, the maximum dispersion of vanadium on SBA-15 has been reported to be 7.2 wt%, corresponding to 2.3 atoms/nm^2 [17]. With 3.1V/nm^2, the surface coverage of the 8V/SBA-15 sample lies above this value. For the 14V/SBA-15 sample with a coverage of 13.6V/nm^2 the presence of V_2O_5 is expected. Surprisingly, the diffractogram of 14V/SBA-15 (not shown) does not show any reflexes and thus excludes the presence of large V_2O_5 crystallites. In its Raman spectrum, however, which is much more sensitive to the presence of three-dimensional vanadia, peaks corresponding to V_2O_5 are present (see below).

Fig. 1 shows the nitrogen adsorption/desorption isotherms for various loadings. The surface area decreases substantially from the blank to the loaded catalysts (Table 1). For the lower loadings this is mainly due to the grafting step [18]. All samples exhibit type IV isotherms with an HI-type hysteresis, indicative for the intact large-pore SBA-15 with one-dimensional cylindrical channels. Even for the heavily loaded sample 14V/SBA-15, the mesopores are not plugged [20], although the surface area is less than 15% of the blank SBA-15 support. The unperturbed pore structure is also visible in the TEM images (not shown). No evidence of crystalline V_2O_5 condensed on the surface is visible. The even distribution of the vanadia is also confirmed by EDX mapping.

Like the surface area, also the pore diameter (Table 1) is reduced upon the initial grafting step in the synthesis. After loading with 2–8 wt% of vanadium, however, the pore diameter remains constant. Only at the highest vanadia concentration it decreases by 3 Å. With the a(1 0 0) spacing from SAXRD (Table 1) and the pore diameter, a mean vanadia-layer thickness can be estimated. For 2V- and 4V/SBA-15 the wall thickness is virtually identical to the blank sample, while it increases to a value of 3 Å for 6–8V/SBA-15, and 6 Å for 14V/SBA-15.

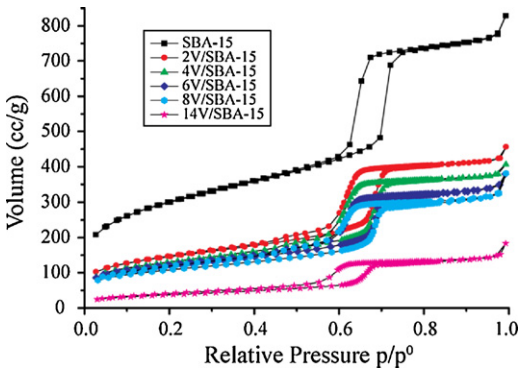

Fig. 1. Adsorption/desorption isotherms (−196 °C) of nitrogen on V/SBA-15 with different vanadium loadings.

3.2. Spectroscopic characterization of the supported vanadia species

The role of water on the dispersion of vanadia on silica has been the topic of many studies [22–25]. Hydrated vanadia species on silica consist of layers of polymerized vanadia with the transition metal in pseudo-octahedral coordination [22]. A water molecule is bound to about every second vanadium atom in a fully hydrated sample [11]. Upon dehydration the species depolymerize and dimers and oligomers of tetrahedrally coordinated VO_4 units are formed. The dehydrated catalysts have been measured by low temperature UV/Vis spectroscopy as shown in Fig. 2. All spectra are characterized by oxygen → vanadium charge transfer (CT) bands. The position of these bands can be used to estimate the coordination and the degree of polymerization of the vanadia species since polymerization of VO_4 and VO_6 units shifts the CT band towards lower energy [22,26]. All hydrated samples (spectra not shown) show transitions at ~260 and ~370 nm, with an absorption tail extending into the visible region. Since the absorption bands of NH_4VO_3 and $NaVO_3$ at 288/363 nm and 281/353 nm, respectively, are assigned to tetrahedrally coordinated polyvanadate [22], the transitions observed for the hydrated samples are indicative for the presence of polymerized vanadia species. In the case of the dehydrated catalysts, one major band is observed for each sample, whose edge and maximum shifts towards lower energies with increased loading (Fig. 2). The presence of just a single CT band at high energy and the rather similar band positions for differently loaded V/silica catalysts (1–10 wt% V on amorphous SiO_2) has been argued to be indicative for the exclusive presence of isolated tetra-

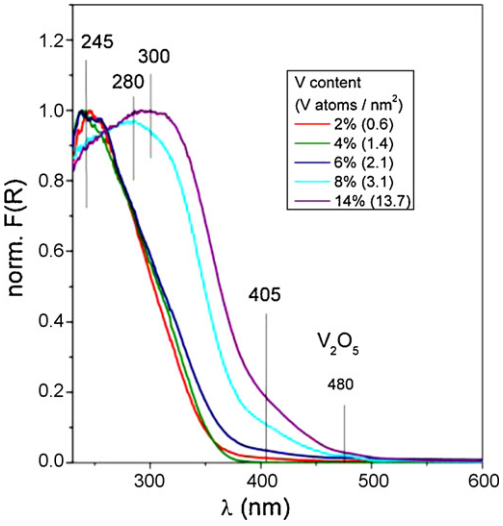

Fig. 2. UV/Vis spectra of dehydrated V/SBA-15 measured at approximately −100 °C.

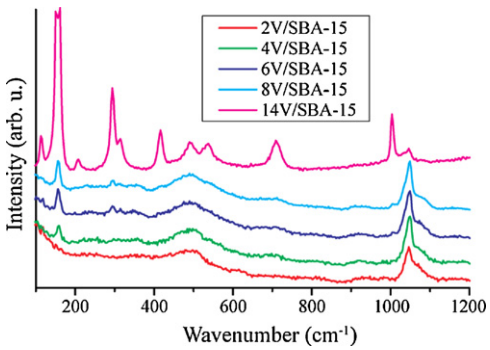

Fig. 3. Raman spectra of dehydrated V/SBA-15 obtained upon excitation with a 488 nm laser. Spectra are offset for clarity. The peak at 155 cm^{-1} for 14V/SBA-15 is cut off to ~1/3 of its real intensity.

hedral O=V(–O–Si)$_3$ species [27,28]. Upon precise inspection of the highly resolved UV/Vis spectra of samples 2–14V/SBA-15, however, it can be seen that the peak in fact consists of at least two transitions centered around 250 and 300 nm. These two peaks have been postulated to be due to isolated V sites as well as oligomeric V–O–V-species [29]. The contribution around 300 nm is dominating in the spectra of the catalysts with loadings >2.1V atoms/nm^2, while at lower loadings the peak maximum is clearly located below 300 nm suggesting the dominance of monomeric species for the catalysts 2–6V/SBA-15 (0.6–2.1V atoms/nm^2). This is in line with findings for vanadia on alumina, where for loadings larger than 1.2V/nm^2, mono- as well as polyvanadates have been observed to coexist. For loadings higher than 4.4V/nm^2 on alumina also some V_2O_5 was present [30,31]. Recent resonant Raman spectroscopy studies with different excitation-laser wavelengths even point to the presence of three different monomeric VO_4 species on alumina at a loading as low as 0.16V/nm^2, although only a single band is resolved in the UV/Vis spectrum [32,33]. The presence of a mixture of different species, including non-monomeric vanadia, has been transmitted also to vanadia on SBA-15, based on near-edge X-ray absorption fine structure (NEXAFS) measurements [34,35]. The shift in the edge energy and adsorption maxima of the dehydrated V/SBA-15 samples in Fig. 2 could thus be due to a changing degree of polymerization. It is known that the electron density of metal oxide domains depends on the particle size. The local electron density decreases for larger particles and the electrons become more delocalized, leading to lower edge energies [36]. In any case, in agreement with XRD, an absorption band near 500 nm, which would indicate the presence of bulk vanadium oxide, has not been found in the UV/Vis spectra, even not for the sample with the highest vanadium loading, but the increase in intensity above 400 nm for 4–14V/SBA-15 suggests progressive polymerization.

The Raman spectra of V/SBA-15 obtained upon excitation with 488 nm light are shown in Fig. 3. The vibrational resonance at 1047 cm^{-1}, dominating the spectra of 2–8V/SBA-15 in Fig. 3, has been argued to be due to the V=O stretch of monovanadate species [9]. It is clear that the peak originates from a monoxo V=O stretch vibration, as revealed by ^{18}O labeling [28,37,38]. However, monomeric and oligomeric vanadia species cannot be discriminated by vibrational spectroscopy since computations predict their V=O stretch vibrations very close together between 1025 and 1050 cm^{-1} [39]. As can be seen in Fig. 3, the peak at 1047 cm^{-1} shows a pronounced shoulder to higher wavenumbers near 1080 cm^{-1}. This shoulder has been claimed to be characteristic for Si–O^- and Si(–O^-)$_2$ functionalities and assigned to perturbed silica vibrations, indicative of the formation of V–O–Si bonds [22,27,28]. However, this band shifts upon ^{16}O–^{18}O isotope exchange although it was found that the silica support vibrations do not appear to have undergone significant isotopic oxygen exchange [28], shading doubt on the above assignment. It cannot be excluded that the band at 1080 cm^{-1} originates from an in-phase V–O–Si vibration [39,40], or, since the intensity ratio of the peaks at 1047 and 1080 cm^{-1} is not constant but increases with increasing vanadium loading, from two vanadyl groups, which are structurally different. For 2–8V/SBA-15, a weak peak around 925 cm^{-1} is visible in the Raman spectra. Its assignment has been the topic of an extensive discussion in literature. Assignments range from V=O stretch vibrations in polymeric vanadia chains [26], to polymeric V–O–V vibrations [37,41], to peroxo O–O stretching vibrations in an umbrella type O=V(O_2)OSi species [42], or to a dihydroxy species O=V(OH)$_2$(O–Sup) with just one vanadium-support bond [43,44]. However, quantum chemical calculations based on density functional theory find V–O–V vibrations to appear below 800 cm^{-1} [39], while the observed V–OH modes were probably due to hydration effects [21]. The band at 925 cm^{-1} is thus assigned to an out-of-phase vanadium–silicon support vibration, in agreement with recent literature [30–33,39]. The presence of three-dimensional (bulk-like) vanadia can be sensitively monitored using Raman spectroscopy, mainly by vibrational resonances at 144, 284, 303, 404, 482, 525, 702 and 994 cm^{-1} [19,22]. All these peaks are visible in the spectrum of 14V/SBA-15 in Fig. 3. The vibrational resonance at 994 cm^{-1} appears also in the spectra of 6V and 8V/SBA-15, the peak at 144 cm^{-1} even in the spectrum of 4V/SBA-15, which is in agreement with the increase in intensity in the UV/Vis spectra above 400 nm. However, one must consider that V_2O_5 is much more Raman active than vanadyl species and only trace amounts of bulk-like vanadia are expected to be present on the catalysts with low vanadia loading, which may result from an incomplete removal of unbound butylammonium decavanadate in the washing step. In the case of 14V/SBA-15, the vibrational resonance at 1047 cm^{-1} proofs the existence of tetrahedral V_xO_y, which probably still constitute the main species. This is in line with the absence of absorption near 500 nm in the UV/Vis spectrum and with the lack of any V_2O_5 reflexes in the diffractogram of 14V/SBA-15.

In summary, bulk-like vanadia species are present, at the most, in trace amounts up to loadings of 3.1V atoms/nm^2 when deposited on SBA-15 with an ion-exchange method. At loadings of 13.6 atoms/nm^2 three-dimensional amorphous V_2O_5 is formed but a substantial amount of vanadia remains highly dispersed in the intact channels of the silica support. The molecular structure of the catalysts does not depend significantly on the loading but the ratio of monomeric and oligomeric vanadia species changes with oligomeric species dominating for vanadia concentrations higher than 2.1V atoms/nm^2 denoting that, most probably, a mixture of monomeric and oligomeric vanadyl coexists on SBA-15 already at a loading of 0.6V atoms/nm^2.

4. Catalytic activity in the ODH of propane

Using a stoichiometric mixture of propane and oxygen in He and a reaction temperature between 380 and 450 °C, a stationary state was reached after 5 min under all conditions and stable performance was observed for the duration of the experiments (12 h). The catalysts were operated in the oxidative regime with a maximum oxygen conversion of 60%. Under these conditions the selectivity decreases with increasing propane conversion for all catalysts (not shown). This is due to the consecutive combustion of C_3H_6 to CO and CO_2, a reaction bearing a lower apparent activation energy than the initial ODH of C_3H_8 [45]. The overall yields (for example ~3% at 430 °C, see Table 2) are considerably lower than reported values for vanadia/SBA catalysts (up to ~30%) [16,29,46]. This can be explained by the lower reaction temperatures in this work as compared to 550 and 650 °C used in the cited studies. A higher

Table 2
Kinetic data for the ODH of propane using V/SBA-15 catalysts[a].

Sample	Selectivity[b] (%)	Activation energy (kJ/mol)	Reaction order propane	Reaction order O_2
2V/SBA-15	60	134 ± 4	1.17 ± 0.05	0.28 ± 0.02
4V/SBA-15	50	141 ± 7	1.22 ± 0.01	0.36 ± 0.05
6V/SBA-1[5]	47	141 ± 6	1.13 ± 0.01	0.35 ± 0.04
8V/SBA-15	44	147 ± 11	1.24 ± 0.01	0.30 ± 0.04
14V/SBA-15	52	151 ± 25	1.30 ± 0.12	0.16 ± 0.04

[a] The errors represent the standard deviation based on 5–7 measurements in the case of activation energies and 2 measurements in the case of reaction orders using two fresh catalyst samples.
[b] At a conversion of 5% at 430 °C.

temperature leads to a higher selectivity [45,47,48], a direct consequence of the lower apparent activation energy of the consecutive deep oxidation. Moreover, gas phase reactions may additionally contribute in a considerable manner to the product spectrum at reaction temperatures above 550 °C. Another explanation could be found in the preparation method of the catalysts used in this study. The reason for the higher selectivity of V/SBA-15 catalysts as compared to vanadia supported for example on MCM-41 was argued to be due to a fast transfer of propene away from the active sites, thus preventing deep oxidation [29,46]. However, in the present work the inner pore diameter of SBA-15 matches the mean diameter of the SBA-15 material studied by Liu et al. [29], even though in the functionalization step of SBA-15, the pore diameter is significantly decreased. Especially the pore diameters of the vanadia containing catalysts are favorably high and decrease only slightly with increasing vanadia content demonstrating the benefits of the V grafting procedure by ion exchange. Reduced mass transfer within the pores might be reflected by the observation that for conversion levels above 4%, the selectivity at constant conversion decreases with increasing vanadium content. However, the selectivity is not clearly related to the pore diameter and the catalyst 14V/SBA-15 shows a dependency other than the catalysts with lower V content suggesting that rather the nature of the active species dominates the shape of the curves.

The only major reaction products are CO, CO_2, and C_3H_6. C_2H_4 (>2% selectivity), acrolein, and acrylic acid formation (both >0.1% selectivity) are not observed in significant amounts, which is in contrast to some earlier studies [11,16,29,49] and possibly due to the lower reaction temperature and due to differences in the feed composition.

Iglesia and co-workers found a selectivity maximum at intermediate vanadia loadings on various supports, which was linked to the prevalence of V–O–V sites [9,47]. In this work no obvious trend is visible from the selectivity reported in Table 2 and all catalysts behave rather similarly, as was noticed for vanadia on an MCM-41 support [50]. This is in line with the finding that for vanadia on SBA-15, the molecular structure of the catalyst does not change significantly with loading.

Table 2 summarizes the kinetic results of V/SBA-15 in the ODH of propane, apparent activation energies and reaction orders. Arrhenius plots yield apparent activation energies between 134 and 151 kJ/mol (Fig. 4). For 2V/SBA-15 (0.6V/nm^2) the value of 134 kJ/mol lies between the experimental activation energies for propane ODH using vanadia/MCM-41 catalyst (122 kJ/mol for >5V/nm^2) [50,51], a calculated value for a silica supported vanadia model catalyst (123 kJ/mol) [51] and a barrier of 146 kJ/mol using 0.3V/nm^2 on amorphous silica [48]. A kinetic investigation for a V/SBA-15 catalyst with 2.7 wt% vanadia yielded a significantly lower apparent activation energy of only 103 kJ/mol [52]. The activation energies measured here are similar for all catalysts. For the low-loaded species an excellent reproducibility is observed for repeated measurements, also when using a fresh catalyst (squares, circles, and triangles in left panel of Fig. 4).

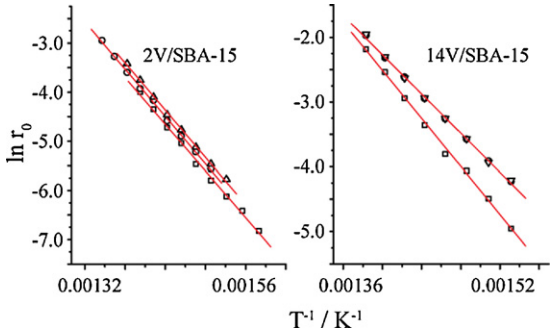

Fig. 4. Arrhenius plots for 2V/SBA-15 and 14V-SBA-15. Three measurements are shown.

The situation is different in the case of 14V/SBA-15. Using a fresh catalyst, a very high apparent activation barrier of ~165 kJ is obtained upon measuring the conversion between 380 and 450 °C (squares in right panel of Fig. 4). In subsequent runs, the activation energy drops to ~140 kJ/mol (triangles and circles in right panel of Fig. 4). While the catalysts 2–8V/SBA-15 are very stable and reproducible in their catalytic performance, 14V/SBA-15 behaves highly dynamic. This must be connected to profound changes in the structural properties of this particular catalyst. 14V/SBA-15 is the only sample, for which a substantial amount of bulk-like V_2O_5 was found to be present, as proven by the Raman spectra. The other samples are characterized by a mixture of monomeric and polymeric vanadyl species of different domain size. Thus, it is not the degree of polymerization of the vanadia species that changes the apparent activation barrier for ODH, but it is obviously the ratio of two-dimensional polymeric species and three-dimensional bulk-like V_2O_5 that plays the crucial role. The importance of monomeric vanadyl species is therefore questioned.

Assuming a first order rate law [45,52], the reaction order of propane is close to one (Table 2). This reflects the participation of propane in the rate determining step, which is the abstraction of the first hydrogen atom [51]. With a value of ~0.3 the reaction order of oxygen is much lower, showing that the reoxidation of the catalyst is fast in comparison to the hydrogen abstraction. Still, the reaction order is not zero, in agreement with previous studies [45,53], and the reoxidation with O_2 is not instantaneous. This could be an explanation for the generally better selectivity of dispersed vanadia as compared to V_2O_5. It is known that a slower reoxidation of the vanadium center, for example by using N_2O instead of O_2, leads to a more selective reaction [50,54]. Interestingly, the reaction order of oxygen decreases for 14V/SBA-15 (Table 2), the sample that is known to contain unselective V_2O_5.

5. Conclusions

The use of an automated laboratory reactor allows for a controlled and reproducible synthesis of SBA-15 supported vanadia

catalysts containing between 0.6 and 13.6V atoms/nm^2. A detailed spectroscopic characterization shows that up to a loading of 3.1V/nm^2 the dehydrated catalysts show similar structures. They all contain a mixture of monomeric and polymeric tetrahedral V_xO_y species. The ratio of monomeric to oligomeric species and their domain size depends on the loading. The catalyst with 13.6V/nm^2 contains not only tetrahedral V_xO_y but also a substantial amount of three-dimensional, bulk-like V_2O_5. The structural similarity of the lower loaded samples is reflected in their catalytic properties in the ODH of propane. The measured activation energies and reaction orders in propane and oxygen do not differ substantially. The clear transition point in the degree of oligomerization between 2V atoms/nm^2, where monomeric vanadia species dominate, and 3V atoms/nm^2, where oligomerized vanadia species are prevailing, is not reflected in qualitative changes in the reactivity. The activation energy of the high-loaded sample changes with reaction conditions, probably reflecting structural changes between amorphous, bulk-like vanadia and two-dimensional, highly dispersed vanadia species during time on stream. It therefore seems that not the presence of monomeric but rather of polymeric vanadia species plays the major role in the activation of propane.

Acknowledgements

We gratefully acknowledge the skilful assistance of D. Brennecke for the catalyst preparation, G. Lorenz for performing the BET measurements, Dr. F. Girgsdies and E. Kitzelmann for the XRD, Dr. G. Auffermann (MPI Dresden) for the ICP-AES, Dr. Di Wang and G. Weinberg for the TEM and SEM, Dr. G. Tzolova-Müller for the UV/Vis spectroscopy, O. Korup, Dr. I. Oprea, and Dr. R. Horn for the Raman spectroscopy. This work was supported by the German Research Foundation (Deutsche Forschungsgemeinschaft, DFG) through the corporate research center "Structure, dynamics and reactivity of transition metal oxide aggregates" (Sonderforschungsbereich 546, http://www.chemie.hu-berlin.de/sfb546).

References

[1] B.M. Weckhuysen, D.E. Keller, Catalysis Today 78 (2003) 25.
[2] A. Bielanski, M. Najbar, Applied Catalysis A: General 157 (1997) 223.
[3] B. Grzybowska-Swierkosz, Applied Catalysis A: General 157 (1997) 263.
[4] P. Forzatti, Heterogeneous Chemistry Reviews 3 (1996) 33.
[5] J.M. López Nieto, Topics in Catalysis 41 (2006) 3.
[6] M. Abon, J.-C. Volta, Applied Catalysis A: General 157 (1997) 173.
[7] B. Solsona, V.A. Zazhigalov, J.M. López Nieto, I.V. Bacherikova, E.A. Diyuk, Applied Catalysis A: General 149 (2003) 81.
[8] F. Cavani, N. Ballarini, A. Cericola, Catalysis Today 127 (2007) 113.
[9] A. Khodakov, B. Olthof, A.T. Bell, E. Iglesia, Journal of Catalysis 181 (1999) 205.
[10] I.E. Wachs, B.M. Weckhuysen, Applied Catalysis A: General 157 (1997) 67.
[11] C. Hess, ChemPhysChem 10 (2009) 319.
[12] I. Muylaert, P. Van Der Voort, Physical Chemistry Chemical Physics 11 (2009) 2826.
[13] D. Zhao, J. Feng, Q. Huo, N. Melosh, G.H. Fredrickson, B.F. Chmelka, G.D. Stucky, Science 279 (1998) 548.
[14] D. Zhao, Q. Huo, J. Feng, B.F. Chmelka, G.D. Stucky, Journal of the American Chemical Society 120 (1998) 6024.
[15] A. Taguchi, F. Schüth, Microporous and Mesoporous Materials 77 (2005) 1.
[16] Y.-M. Liu, Y. Cao, K.-K. Zhu, S.-R. Yan, W.-L. Dai, H.-Y. He, K.-N. Fan, Chemical Communications (2002) 2832.
[17] C. Hess, H.J.D.T.D. Tilley, Journal of Physical Chemistry B 108 (2004) 9703.
[18] C. Hess, U. Wild, R. Schlögl, Microporous and Mesoporous Materials 95 (2006) 339.
[19] G. Du, S. Lim, M. Pinault, C. Wang, F. Fang, L. Pfefferle, G.L. Haller, Journal of Catalysis 253 (2008) 74.
[20] P. Van Der Voort, P.I. Ravikovitch, K.P. De Jong, A.V. Neimark, A.H. Janssen, M. Benjelloun, E. Van Bavel, P. Cool, B.M. Weckhuysen, E.F. Vansanta, Chemical Communications (2002) 1010.
[21] D.E. Keller, T. Visser, F. Soulimani, D.C. Koningsberger, B.M. Weckhuysen, Vibrational Spectroscopy 43 (2007) 140.
[22] X. Gao, S.R. Bare, B.M. Weckhuysen, I.E. Wachs, Journal of Physical Chemistry B 102 (1998) 10842.
[23] C. Hess, R. Schlögl, Chemical Physics Letters 432 (2006) 139.
[24] C. Hess, G. Tzolova-Muller, R. Herbert, The Journal of Physical Chemistry C 111 (2007) 9471.
[25] C. Hess, Journal of Catalysis 248 (2007) 120.
[26] M. Schraml-Marth, A. Wokaun, M. Pohl, H.-L. Krauss, Journal of the Chemical Society, Faraday Transactions 87 (1991) 2635.
[27] E.L. Lee, I.E. Wachs, The Journal of Physical Chemistry C 111 (2007) 14410.
[28] E.L. Lee, I.E. Wachs, The Journal of Physical Chemistry C 112 (2008) 6487.
[29] Y.-M. Liu, Y. Cao, N. Yi, W.-L. Feng, W.-L. Dai, S.-R. Yan, H.-Y. He, K.-N. Fan, Journal of Catalysis 224 (2004) 417.
[30] Z. Wu, H.-S. Kim, P.C. Stair, S. Rugmini, S.D. Jackson, Journal of Physical Chemistry B 109 (2005) 2793.
[31] Z. Wu, P.C. Stair, S. Rugmini, S.D. Jackson, The Journal of Physical Chemistry C 111 (2007) 16460.
[32] H.-S. Kim, P.C. Stair, The Journal of Physical Chemistry A 113 (2009) 4346.
[33] H.-S. Kim, S.A. Zygmunt, P.C. Stair, P. Zapol, L.A. Curtiss, The Journal of Physical Chemistry C 113 (2009) 8836.
[34] M. Cavalleri, K. Hermann, A. Knop-Gericke, M. Hävecker, R. Herbert, C. Hess, A. Oestereich, J. Döbler, R. Schlögl, Journal of Catalysis 262 (2009) 215.
[35] M. Hävecker, M. Cavalleri, R. Herbert, R. Follath, A. Knop-Gericke, C. Hess, K. Hermann, R. Schlögl, Physica Status Solidi B 246 (2009) 1459.
[36] R.S. Weber, Journal of Catalysis 151 (1995) 470.
[37] B.M. Weckhuysen, J.-M. Jehng, I.E. Wachs, Journal of Physical Chemistry B 104 (2000) 7382.
[38] G. Busca, Journal of Raman Spectroscopy 33 (2002) 348.
[39] N. Magg, B. Immaraporn, J.B. Giorgi, T. Schroeder, M. Bäumer, J. Döbler, Z. Wu, E. Kondratenko, M. Cherian, M. Baerns, P.C. Stair, J. Sauer, H.-J. Freund, Journal of Catalysis 226 (2004) 88.
[40] J. Döbler, M. Pritzsche, J. Sauer, The Journal of Physical Chemistry C 113 (2009) 12454.
[41] L.J. Burcham, G. Deo, X. Gao, I.E. Wachs, Topics in Catalysis 11/12 (2000) 85.
[42] O.L.J. Gijzeman, J.N.J. van Lingen, J.H. van Lenthe, S.J. Tinnemans, D.E. Keller, B.M. Weckhuysen, Chemical Physics Letters 397 (2004) 277.
[43] D.E. Keller, F.M.F. de Groot, D.C. Koningsberger, B.M. Weckhuysen, Journal of Physical Chemistry B 109 (2005) 10223.
[44] D.E. Keller, D.C. Koningsberger, B.M. Weckhuysen, Journal of Physical Chemistry B 110 (2006) 14313.
[45] B. Frank, A. Dinse, O. Ovsitser, E.V. Kondratenko, R. Schomäcker, Applied Catalysis A: General 323 (2007) 66.
[46] Y.-M. Liu, W.-L. Feng, T.-C. Li, H.-Y. He, W.-L. Dai, W. Huang, Y. Cao, K.-N. Fan, Journal of Catalysis 239 (2006) 125.
[47] M.D. Argyle, K. Chen, A.T. Bell, E. Iglesia, Journal of Catalysis 208 (2002) 139.
[48] A. Dinse, B. Frank, C. Hess, D. Habel, R. Schomäcker, Journal of Molecular Catalysis A: Chemical 289 (2008) 28.
[49] B. Solsona, T. Blasco, J.M.L. Nieto, M.L. Pena, F. Rey, A. Vidal-Moya, Journal of Catalysis 203 (2001) 443.
[50] E.V. Kondratenko, M. Cherian, M. Baerns, D. Su, R. Schlögl, X. Wang, I.E. Wachs, Journal of Catalysis 234 (2005) 131.
[51] X. Rozanska, R. Fortrie, J. Sauer, Journal of Physical Chemistry C 111 (2007) 6041.
[52] A. Dinse, S. Khennache, B. Frank, C. Hess, R. Herbert, S. Wrabetz, R. Schlögl, R. Schomäcker, Journal of Molecular Catalysis A: Chemical 307 (2009) 43.
[53] A. Bottino, G. Capannelli, A. Comite, S. Storace, R. Di Felice, Chemical Engineering Journal 94 (2003) 11.
[54] O. Ovsitser, M. Cherian, E.V. Kondratenko, The Journal of Physical Chemistry C 111 (2007) 8594.